Available online at www.sciencedirect.com

ScienceDirect

Ceramics International 41 (2015) 8064–8069

CERAMICS INTERNATIONAL

www.elsevier.com/locate/ceramint

Reaction sintering of kaolin-natural phosphate mixtures

F. Chouia[a,b], H. Belhouchet[a,c,*], F. Sahnoune[c], F. Bouzrara[b]

[a]*Non Metallic Materials Laboratory, University of Ferhat Abbas Sétif 1, Sétif 19000, Algeria*
[b]*Département de Physique, Faculté des sciences exactes et informatique, Université de Jijel, Jijel 18000, Algeria*
[c]*Physics Department, Faculty of Science, University Mohamed Boudiaf of M'sila, 28000 M'sila, Algeria*

Received 17 December 2014; received in revised form 11 February 2015; accepted 2 March 2015
Available online 9 March 2015

Abstract

Low-cost materials based on hydroxyapatite (HAp), anorthite and mullite were prepared from mixtures of Algerian kaolin (DD2) and natural phosphate (NP). Three different compositions (20 K, 50 K and 80 K) with 20, 50 and 80 wt% Kaolin were studied. In the 20 K samples (with 80% natural phosphate), HAp based ceramics were obtained by the solid-state reaction (SSR). Anorthite–HAp composites were formed at 1100 °C in the 50 K samples remaining stable up to 1300 °C. The primary mullitization occurred by SSR in the 80 K sample at 1000 °C followed by formation of anorthite from the phosphate dissolution. These results show that the reaction sintering of kaolin/phosphate mixtures is a feasible route to obtain HAp, anorthite materials that can be used in electronics industry, industrial heat exchangers and biomedical applications.

Keywords: B. Composites; Kaolin (DD2); Natural phosphate; Reaction-sintering

1. Introduction

During the last few decades, intensive research has been conducted with the aim of producing hydroxyapatite (HAp) biomaterials of desired biological, physicochemical, and mechanical properties [1]. They have been considered as representative materials for bone grafts due to their similarities to the bone apatite [2]. HAp materials are also used for separation and purification of proteins and in drug delivery systems [3]. Anorthite is an economical ceramic that has good physical properties such as low thermal expansion coefficient, high thermal shock resistance and low dielectric constant. With these excellent characteristics, the anorthite ceramics are applied in electronics industry, heat exchangers and biomedical materials [4,5].

The sintering of Algerian kaolin nuances known as (DD1, DD2 and DD3) from Djebel Debbagh has been studied by some researchers [6–8]. Natural phosphate is a general term that describes naturally occurring mineral assemblages containing a high concentration of phosphate minerals. About 80 wt% of world natural phosphate production is derived from deposits of sedimentary marine origin mainly composed of apatite's [9].

Algeria has important phosphate reserves located in the east of the country at Djebel Onk. Natural phosphates have also largely been studied [10,11]. To our knowledge, the sintering reaction between kaolin and natural phosphate has not been treated.

The objective of this study was to produce inexpensive ceramics based on hydroxyapatite, anorthite and mullite starting from mixtures of two very abundant local raw materials: kaolin (DD2) and natural phosphate (NP).

2. Materials and methods

Two raw materials were used in this study:

1. Kaolin (DD2) from Djebel Dbag in Guelma.
2. Natural phosphate (NP) from the mine of Djebel Onk (East of Algeria).

---

[*] Corresponding author at: Non Metallic Materials Laboratory, University of Ferhat Abbas Sétif 1, Sétif 19000, Algeria Tel.: +213 665618919.
E-mail address: hbelhou@yahoo.com (H. Belhouchet).

http://dx.doi.org/10.1016/j.ceramint.2015.03.003
0272-8842/

Their chemical compositions are given in Table 1.

Three compositions were prepared by varying the percentage of the kaolin (20, 50 and 80%). These are named 20 K, 50 K and 80 K respectively. The powders were milled through planetary ball milling (Fritsch P6) for 5 h. The slurry was dried at 110 °C, powdered and sieved through a 63 µm mesh, then compacted at a pressure of 75 MPa using a cold uniaxial press. Cylindrical specimens of 13 mm diameter were produced. The mixtures powders were sintered under normal conditions during 2 h at temperatures between 1000 and 1400 °C. XRD analyses were carried out using a Bruker D8 diffractometer. The XRD tests conditions were Ni-filtered $Cu_{k\alpha}$ X radiation (35 kV–30 mA) with a scanning speed of 37° (2θ) per minute and at an increment of 0.05°. The chemical functional groups were investigated by Fourier transform infrared spectroscopy (FT-IR) Shimadzu Corporation type FT-IR 8300 E within the wave number range of 4000–400 cm^{-1}. DTA was conducted in the temperature range of 25–1200 °C under static air. A mass of 40 mg of powders mixture was heated at rate of 10 °C/min by Setaram DTA 92 thermal analysis system. The bulk density and open porosity of fired samples were determined by the Archimedes method using distilled water. The morphology of the samples was observed by scanning electronic microscopy SEM (JEOL JSM-7001F).

Table 1
Chemical composition of kaolin (DD2) and natural phosphate (NP).

Elements	SiO_2	Al_2O_3	CaO	P_2O_5	Fe_2O_3	Na_2O	SO_3	K_2O	MgO	L.O.I
DD2	45.52	38.75	0.18	–	0.04	0.05	–	0.03	–	15.44
NP	02.30	0.41	53.16	26.74	0.69	0.85	3.26	0.10	0.75	11.74

3. Results and discussion

We characterized the obtained materials using XRD, FT-IR, DTA, open porosity, apparent density and SEM analysis. The XRD patterns of the sintered samples at different temperatures are shown in Fig. 1. The samples 20 K show the presence of HAp at 1000 °C (Fig. 1(a)). In addition to the HAp, this spectra reveals the presence of anorthite. Above 1200 °C, the intensity of anorthite increases with temperature up to 1300 °C and decreases at 1400 °C. This is due to the dissolution of this phase in the HAp matrix.

The XRD spectra corresponding to 50 K sample (Fig. 1(b)) shows a notably decrease in HAp intensity in the temperature range (1000–1200 °C). Simultaneously with the decreases of the peaks corresponding to HAp, the anorthite intensity increases. A new phase of β-TCP was detected in these samples at 1300 °C [12].

The XRD patterns recorded from the samples 80 K (Fig. 1(c)) shows the presence of cristobalite at 1000 °C whose intensity increases at 1100 °C and then disappears at 1300 °C. We notice the presence of small peaks corresponding to HAp between 1000 and

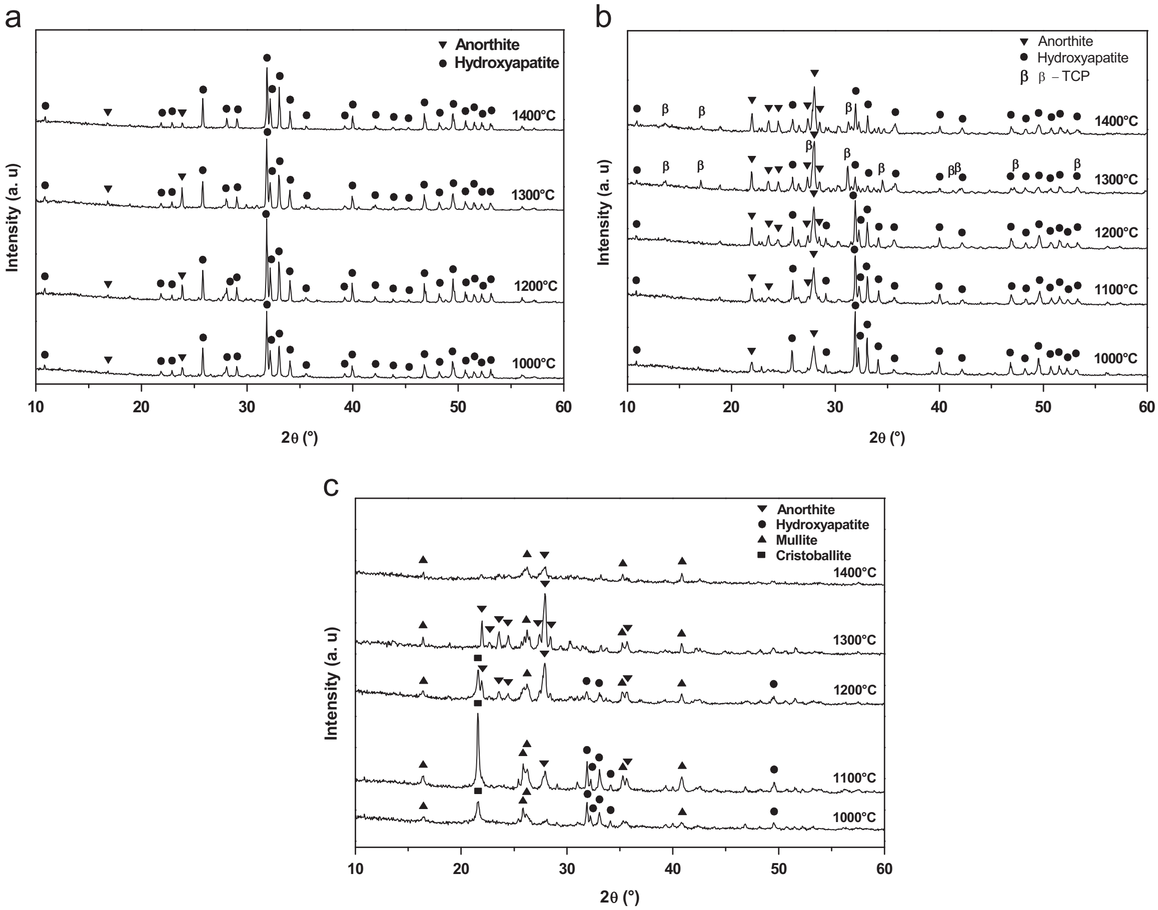

Fig. 1. XRD patterns of the samples sintered at different temperatures for 2 h: (a) 20 K, (b) 50 K, and (c) 80 K.

1100 °C. At 1100 °C, the anorthite phase was formed with an increasing intensity up to 1300 °C. The formation of this anorthite, resulting from the reaction between kaolin and CaO, comes from NP dissociation. In these samples, a new phase (Mullite) appeared between 1000 and 1300 °C. At 1400 °C, a total disappearance of all phases is obtained by fusion. HAp–anorthite composites were formed in the cases of 20 K and 50 K samples. In the 80 K samples where kaolin is in excess, anorthite–mullite composites were revealed.

Furthermore, based on their FT-IR spectra (Fig. 2), the samples 20 K (Fig. 2(a)) heated at 1100, 1200 and 1300 °C show two bands located at 424 and 686 cm^{-1} relating to the bond Si–O vibrations [13,14]. Another band was observed at 470 cm^{-1} corresponding to the deformation of Si–O band. The observed peaks at 1045 cm^{-1} demonstrate the presence of HAp: υ_3 PO$_4^{3-}$ [2]. There were also two other sharp peaks at 570–600 cm^{-1} for the υ_4 O–P–O bond and at 925 cm^{-1} for υ_4 non-degenerate P–O symmetric stretching [15,16]. The last broad band located at 1153 cm^{-1} corresponds to the υ_{as} PO$_2^{3-}$ vibrations. At 1400 °C, the majority of the bands disappeared except for the two bands at 600 and 1045 cm^{-1} (υ_3 PO$_4^{3-}$) which become larger with less intensity.

In the 50 K samples (Fig. 2(b)), there is a clear modification of the functional groups. We can notice the appearance of new band at 1110 cm^{-1} corresponding to Si–O in the sample heated at 1000 °C [13]. In the sample heated at 1100 °C, wide peaks were found at 588 cm^{-1} for υ_4 PO$_4^{3-}$ bond, 679 cm^{-1} for Si–O band, 746 cm^{-1} for Si–O–Al band and at 1045 cm^{-1} for υ_3 PO$_4^{3-}$. At 1300 °C, the intensity of the peak at 1045 cm^{-1} (υ_3 PO$_4^{3-}$) increases due to the formation of the tricalcium phosphate ($Ca_3(PO_4)_2$) (TCP). Only two bands 600 and 1045 cm^{-1} (υ_3 PO$_4^{3-}$) appeared at 1400 °C.

In the 80 K samples, the bands corresponding to the PO$_4^{-3}$ groups (600 and 1045 cm^{-1}) tend to disappear (Fig. 2(c)) between 1100 and 1300 °C. Only small bands of residual PO$_4^{3-}$ groups (472 and 570 cm^{-1}) were present in the samples heated at 1100 and 1200 °C. Two peaks at 679 and 761 cm^{-1} were observed corresponding to Si–O bond vibrations. The new strong band at 1097 cm^{-1} is related to the hybrid AlO$_4$vibrations. The disappearance of the majority of the bands at 1400 °C is caused by the fusion of the materials.

Fig. 3 shows typical DTA curves of samples heated from room temperature to 1200 °C at a heating rate of 10 °C/min. On the curve of 20 K samples two clear endothermic peaks are

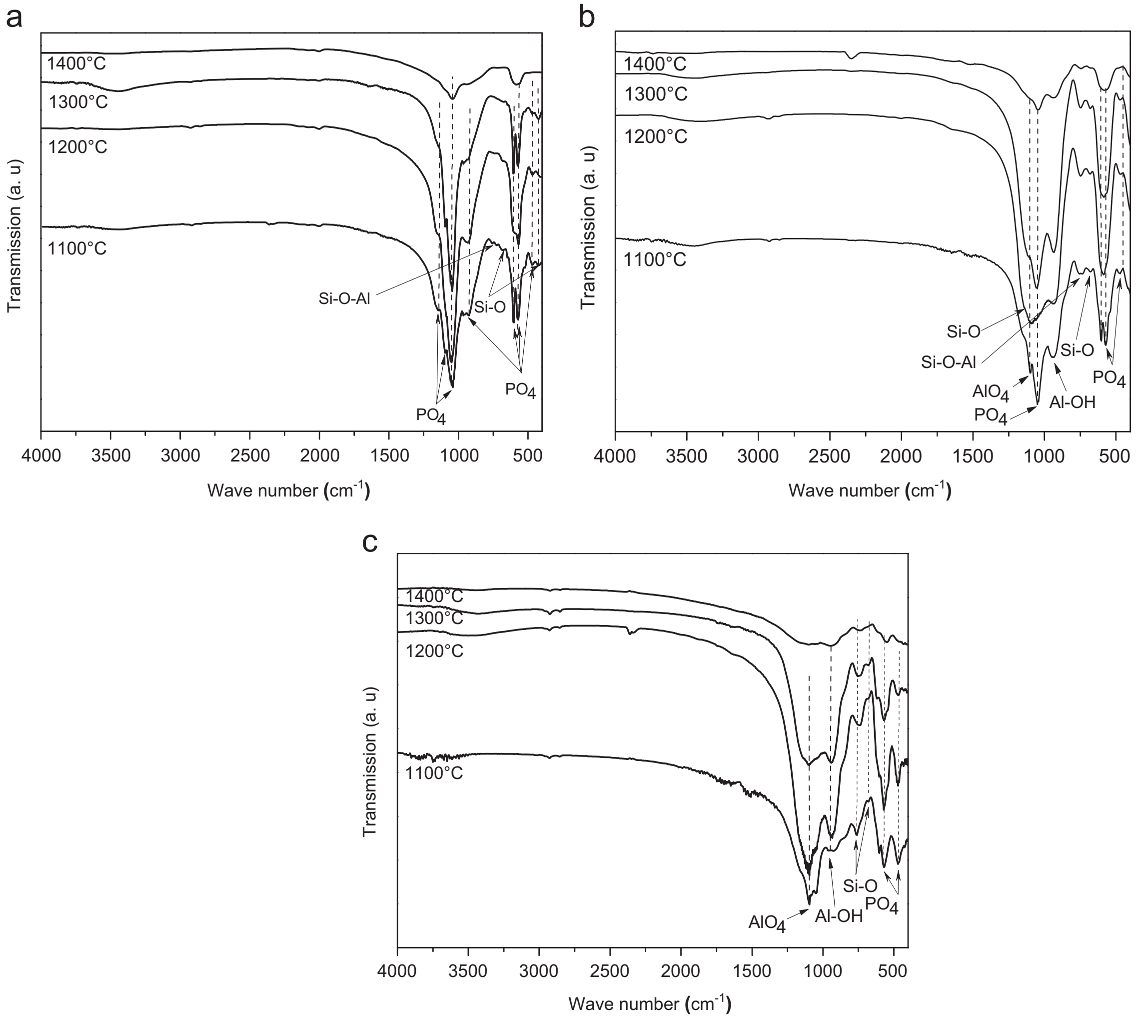

Fig. 2. FT-IR spectra of the samples sintered at different temperatures for 2 h: (a) 20 K, (b) 50 K, and (c) 80 K.

observed at 124 and 546 °C. The first one is due to the evaporation of adsorbed water, while the second peak is due to the dehydration of the kaolinite [17,18]. Furthermore, an endothermic peak is present at about 755 °C which may be due to the thermal decomposition of $CaCO_3$ into CaO and CO_2 [19]. Two exothermic peaks observed at 732 °C and 931 °C: first one is due to the partial crystallization of HAp [20,21], while the second latter indicates some order in a crystalline formation. Such crystalline formation was attributed either to a spinel formation or others attributed it to mullite nucleation [8,17,18]. Three small endothermic peaks are observed around 1039, 1137 and 1194 °C and may due to the decomposition of HAp.

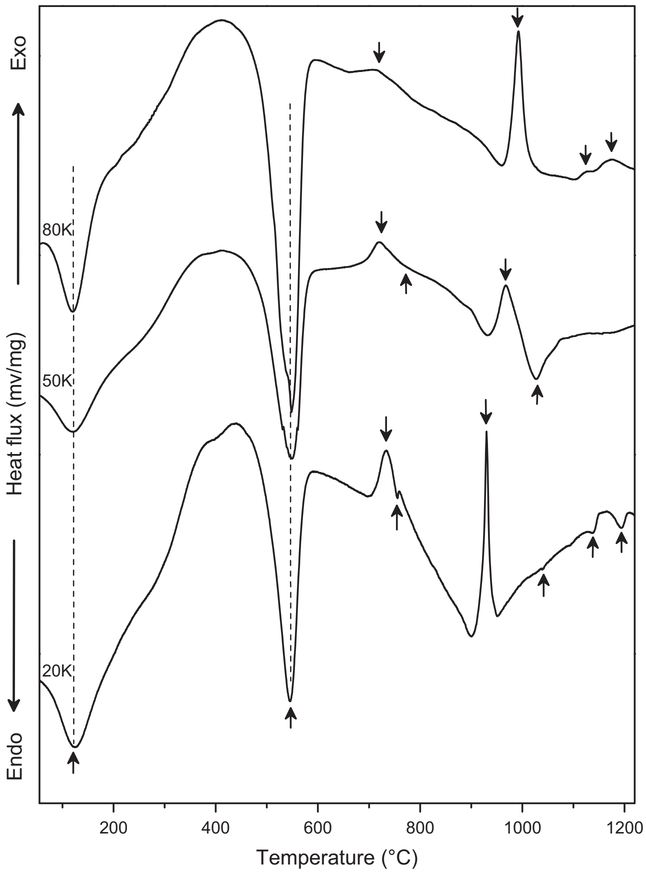

Fig. 3. DTA curves for kaolin-natural phosphate mixtures during heating.

The exothermic and endothermic peaks appeared at about 732 °C and 755 °C, respectively are decrease for 50 K samples and become absent for 80 K samples. Further, the three peaks observed in 20 K sample are absent in both 50 K and 80 K samples, due to the decrease of NP amount in the mixture. The exothermic peak at about 931 °C in the DTA curve of 50 K and 80 K samples is shifted upward to 967 °C and 992 °C, respectively. The shift can be explained by the decrease of NP amount compared to kaolin. The CaO, produced during carbonates decomposition, acts as fluxing agents when reducing the difference between initial and maximum sintering temperatures [22]. There is also a sharp endothermic peak at about 1027 °C for 50 K sample which is absent in the two DTA curves. This peak can be attributed to the liquidus temperature or melting temperature of crystalline phases. The large broad and small exothermic peaks observed for 80 K samples in the region 1000–1200 °C may be related to the secondary mullite formation and cristobalite crystallization from kaolinite [18].

The curves of the open porosity and apparent density variation with kaolin content have different aspects according to the sintering temperature (Fig. 4). The results indicate that the sample 20 K has significant difference compared with samples 50 K and 80 K. At first, for 20 K the open porosity values decrease progressively between 900 and 1100 °C. At high sintering temperatures, above 1200 °C a large amount of open porosity are completely closed [23]. However, CO_2 comes from decarbonation of $CaCO_3$ is filling in the pores leading to the increase in apparent density with a higher value (2.78 g/cm^3) at 1200 °C (Fig. 4(b)).

A gradual increase in the open porosity is observed also for 50 K samples and is probably due to release of CO_2 outside the sample. The viscosity of glassy phase is largely reduced by CaO coming from the dissociation of HAp with increase of temperatures. The low viscosity facilitates the CO_2 escape

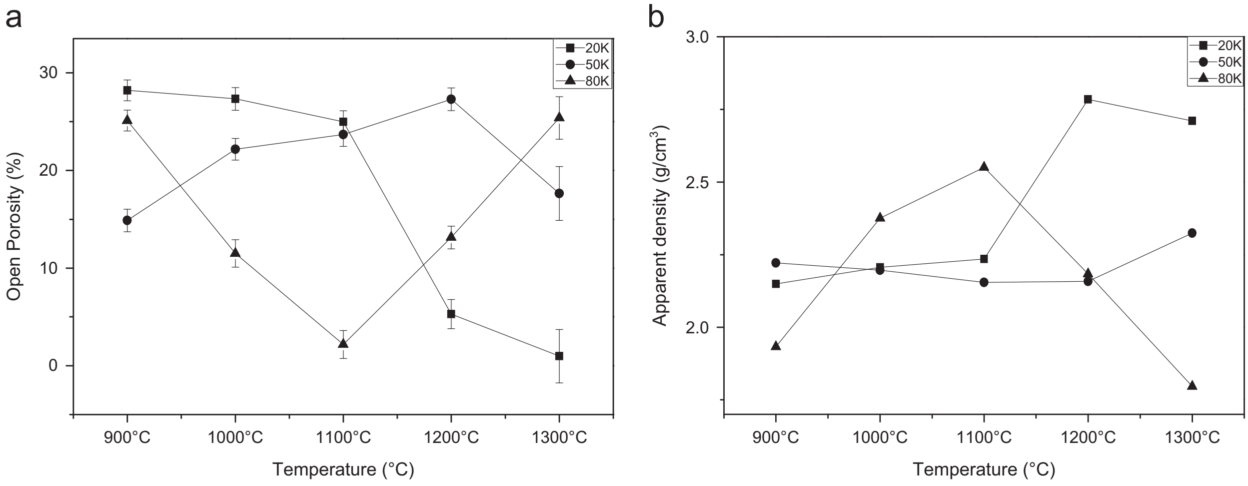

Fig. 4. Open porosity (a) and apparent density (b) of the samples sintered at different temperatures for 2 h.

from pores [24]. A steady diminution in apparent density is observed when the sintering temperature is raised from 900 to 1000 °C. The apparent density is stabilized for temperatures above 1100 °C. For higher sintering temperature (1300 °C) a slight increase of the apparent density was observed (reached the maximum value of 2.32 g/cm^3). This is attributed to the formation of the tricalcium phosphate (β-TCP) beyond 1200 °C, which has been confirmed by the phase analysis using XRD. The curve of 80 K sample shows a decrease of open porosity from 900 to 1100 °C and can be attributed to the formation of cristobalite phase. It is known to have a large coefficient of thermal expansion which affects strongly the porous ceramics. By increasing of the temperature, the open porosity increases and can be attributed to fluxing of cristobalite phase. The higher apparent density is attributed to the existence of cristobalite in the glass matrix.

The microstructures shown in Fig. 5 corresponds to the three mixtures fired at 1300 °C during 2 h. According to the literature [4,25,26], the micrograph corresponding to 20 K sample shows very high HAp grains with elongated forms (Fig. 5(a)). On the other hand, the 50 K sample microstructure (Fig. 5(b)) reveals enlarged anorthite grains and fine particles of β-TCP between the coarse grains. The 80 K sample microstructure shows irregularly shaped large anorthite grains and round-shaped mullite grains distributed in the anorthite matrix.

4. Conclusion

The results of the reaction sintering of the studied kaolin-natural phosphate mixtures (20 K, 50 K and 80 K) indicate the formation of HAp–anorthite composites in 20 K and 50 K samples. β-TCP was formed at 1300 °C in the 50 K samples. In the cases where kaolin is in excess (80 K), anorthite–mullite composites were revealed. From this study, some possibilities of sintering reactions between kaolin and natural phosphate are highlighted.

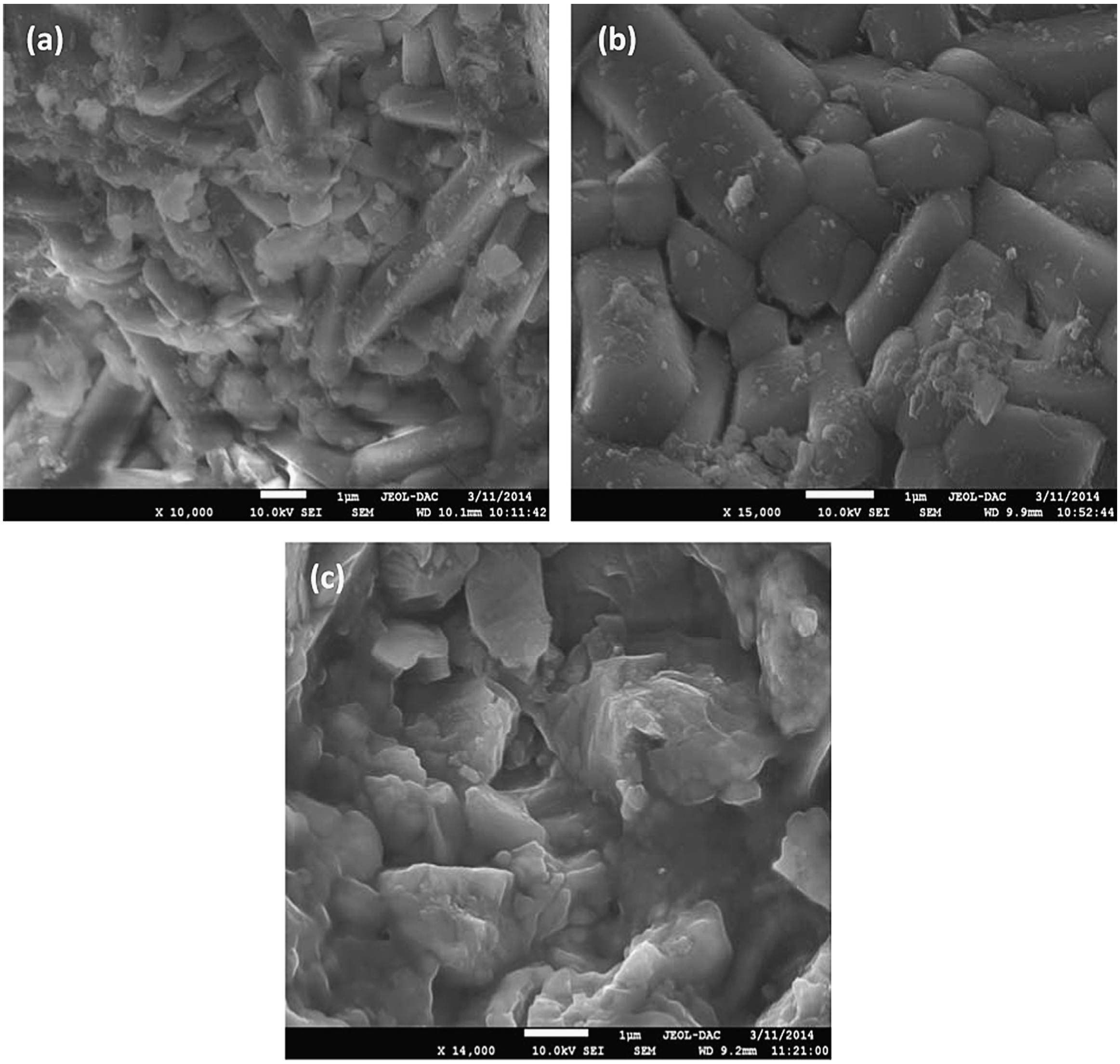

Fig. 5. SEM micrographs of the samples sintered at 1300 °C for 2 h: (a) 20 K,(b) 50 K, and (c) 80 K.

References

[1] A. Sobczak-Kupiec, Z. Wzorek, The influence of calcination parameters on free calcium oxide content in natural hydroxyapatite, Ceram. Int. 38 (2012) 641–647.

[2] J.S. Cho, J.C. Lee, S.H. Chung, J.K. Seo, S.H. Rhee, Effect of grain size and density of spray-pyrolyzed hydroxyapatite particles on the sinterability of hydroxyapatite disk, Ceram. Int. 40 (2014) 6691-6667.

[3] T. Mandal, B.K. Mishra, A. Garg, D. Chaira, Optimization of milling parameters for the mechanosynthesis of nanocrystalline hydroxyapatite, Powder Technol. 253 (2014) 650–656.

[4] X. Cheng, S. Ke, Q. Wang, H. Wang, A. Shui, P. Liu, Fabrication and characterization of anorthite-based ceramic using mineral raw materials, Ceram. Int. 38 (2012) 3227–3235.

[5] S. Kurama, E. Ozel, The influence of different CaO source in the production of anorthite ceramics, Ceram. Int. 35 (2009) 827–830.

[6] F. Bouzerara, A. Harabi, S. Achour, A. Larbot, Porous ceramic supports for membranes prepared from kaolin and doloma mixtures, J. Eur. Ceram. Soc. 26 (2006) 1663–1671.

[7] A. Mecif, J. Soro, A. Harabi, J.P. Bonnet, Preparation of ‚mullite- and zircon-based ceramics using kaolinite and zirconium oxide: a sintering study, J. Am. Ceram. Soc. 93 (2010) 1306–1312.

[8] A. Harabi, F. Zenikheri, B. Boudaira, F. Bouzerara, A. Guechi, L. Foughali, A new and economic approach to fabricate resistant porous membrane supports using kaolin and $CaCO_3$, J. Eur. Ceram. Soc. 34 (2013) 1329–1340.

[9] L. EL-Gaini, A. Meghea, M. Bakasse, Phototransformation of pesticide in the presence of moroccan natural phosphate in aqueous solution, J. Optoelectron. Adv. Mater. 12 (2010) 1981–1985.

[10] K. Rida, B. Chemmal, A. Boukhemkhem, Removal of methylene blue from aqueous solution by natural phosphate, J. Optoelectron. Adv. Mater. 13 (2013) 493–500.

[11] N. Bezzi, D. Merabet, N. Benabdeslem, H. Arkoub, Caractérisation physico–chimique du minerai de phosphate de bled el hadba-Tebessa, Ann. Chim. Sci. Mater. 26 (2001) 5–23.

[12] R.G. Carrodeguas, S. De Aza, α-Tricalcium phosphate: synthesis, properties and biomedical applications, Acta Biomater. 7 (2011) 3536–3546.

[13] R.D. Sahnoun, J. Bouaziz, Sintering characteristics of kaolin in the presence of phosphoric acid binder, Ceram. Int. 38 (2012) 1–7.

[14] S.Q. Yang, P. Yuan, H.P. He, Z.H. Qin, Q. Zhou, J.X. Zhu, D. Liu, Effect of reaction temperature on grafting of γ-aminopropyl triethoxysilane (APTES) onto kaolinite, Appl. Clay Sci. 62–63 (2012) 8–14.

[15] G. Ahn, J.Y. Lee, D.W. Seol, S.G. Pyo, D. Lee, The effect of calcium phosphate cement-silica composite materials on proliferation and differentiation of pre-osteoblast cells, Mater. Lett. 109 (2013) 302–305.

[16] S. Mukherjeea, B. Kundu, S. Sen, A. Chanda, Improved properties of hydroxyapatite-carbon nanotube biocomposite: mechanical, in vitro bioactivity and biological studies, Ceram. Int. 40 (2014) 5635–5643.

[17] F. Sahnoune, M. Chegaar, N. Saheb, Algerian kaolinite used for mullite formation, App. Clay Sci. 38 (2008) 304–310.

[18] A.K. Chakraborty, DTA study of preheated kaolinite in the mullite formation region, Thermochim. Acta 398 (2003) 203–209.

[19] Z. Graba, S. Hamoudi, D. Bekka, N. Bezzi, R. Boukherroub, Influence of adsorption parameters of basic red dye 46 by the rough and treated Algerian natural phosphates, J. Ind. Eng. Chem. (2015) In Press, http://dx.doi.org/10.1016/j.jiec.2014.10.039.

[20] G.C. Koumoulidis, A.P. Katsoulidis, A.K. Ladavos, Preparation of hydroxyapatite via microemulsion route, Coll Interface Sci. 259 (2003) 254–260.

[21] G. Bolelli, D. Bellucci, V. Cannillo, Suspension thermal spraying of hydroxyapatite: microstructure and in vitro behavior, Mater. Sci. Eng. 34 (2014) 287–303.

[22] E. Kłosek-Wawrzyn, J. Małolepszy, P. Murzyn, Sintering behavior of kaolin with calcite, in: Proceedings of the 11th International Conference on Modern Building Materials, Structures and Techniques, MBMST 2013, Procedia Engineering, 57 (2013) pp. 572–582.

[23] K.A. DeFriend, M.R. Wiesner, A.R. Barron, Alumina and aluminate ultra-filtration membranes derived from alumina nanoparticles, J. Membr Sci. 224 (2003) 11–28.

[24] L. Boilet, M. Descamps, E. Rguiti, Processing and properties of transparent hydroxyapatite and β tricalcium phosphate obtained by HIP process, Ceram. Int. 39 (2013) 283–288.

[25] S. Ke, X. Cheng, Y. Wang, Q. Wang, H. Wang, Dolomite, wollastonite and calcite as different CaO sources in anorthite-based porcelain, Ceram. Int. 39 (2013) 4953–4960.

[26] Y. Hana, C. Lia, C. Biana, S. Lia, C.A. Wan, Porous anorthite ceramics with ultra-low thermal conductivity, J. Eur. Ceram. Soc. 33 (2013) 2573–2578.